ISSN 1995-0780, Nanotechnologies in Russia, 2011, Vol. 6, Nos. 1–2, pp. 88–95. © Pleiades Publishing, Ltd., 2011.
Original Russian Text © I.V. Ionova, M.V. Alfimov, V.A. Livshits, 2011, published in Rossiiskie Nanotekhnologii, 2011, Vol. 6, Nos. 1–2.

Adsorption and Molecular Dynamics of Spin Probes on Hydrophobizated Silica Gel Microparticles: EPR Spin-Label Study

I. V. Ionova, M. V. Alfimov, and V. A. Livshits

Photochemistry Center, Russian Academy of Sciences, ul. Novatorov 7a, Moscow, 117419 Russia
e-mail: livsh@photonics.ru

Received June 22, 2010; in final form, September 8, 2010

Abstract—The molecular dynamics parameters and hydrophobicity of the surface of Silasorb silica gel particles covalently modified with alkyl C_nH_{2n+1} groups differing in length ($n = 2, 8, 18$) were studied by electron paramagnetic resonance using spin probes of different structures, sizes, and electrical charges. It has been shown that the hydrocarbon shells of the silica gel microparticles in liquid suspensions provide high rotational and conformational mobility and a very high hydrophobicity of the environment for the incorporated molecules. Some regularities in the dependences of the rotational mobility, orientation ordering, and environmental hydrophobicity have on the hydrocarbon shell thickness have been established for spin probes of different structures: a radical containing an aromatic residue which models a fluorescent sensor molecule, lipid spin probes sensitive to the microviscosity and orientation ordering, and positively charged probes sensitive to electrostatic interactions. It has been found that the rotational mobility of the lipid spin probes sharply decreases upon removing the solvent and recovers in the presence of water or water–ethanol vapors. The high values of rotational mobility and environmental hydrophobicity for the spin probes located in the hydrocarbon shell of the Silasorb particles, which are dispersed in suspensions or in the solvent vapors, allow one to conclude that these microparticles can be perspective matrices for molecular optical chemosensors for analytes in solutions or the gas phase.

DOI: 10.1134/S1995078011010071

INTRODUCTION

Recently, there has been a lot of interest in functional micro- or nanoparticles built on the basis of silicon dioxide. They are used as fluorescent nanosize materials, sorbents in high-efficiency liquid chromatography, and chemo- and biosensors [1–8]. The advantage that silicon dioxide nanoparticles have as matrices for the formation of such materials is that their physical and chemical stability are higher than that of organic polymeric matrices and, at the same time, it is possible to modify the external surface with functional groups. The most important requirements for the production and optimization of the chemosensor materials are (1) a very high molecular and conformational mobility of both the molecular sensor itself and molecules–analytes to make complexation possible and (2) a high hydrophobicity of the environment of the optical sensor to achieve a high fluorescence quantum yield.

One promising way to achieve this aim can be to modify the silica gel surface with alkyl groups. The saturated hydrocarbon chains in which the fast trans-gauche isomerization occurs at conventional temperatures can result in a quasi-liquid structure on the surface of the solid SiO_2 particles with a low dielectric permittivity.

In this work, Silasorb microparticles, the surface of which was covalently modified with hydrocarbon chains with different numbers of carbon atoms (2, 8, 18) bound via a linker, have been used as materials which can have such properties.

These materials were used as sorbents for high-efficiency liquid chromatography in a series of publications [9, 10]. However, they were not used as microplatforms for the production of chemosensors. We used the spin probe method for our investigation. It is well known that this method is highly sensitive to the molecular rotation and polarity (hydrophobicity) of the local environment, and it is also characterized by a high spectral resolution when studying heterogeneous chemical and biological systems [11–17].

MATERIALS AND METHODS

Spherical sorbents on the basis of the Silasorb silica gel (Lachema, Czech Republic) with alkyl groups on the surface with 2 (C-2), 8 (C-8), and 18 (C-18) carbon atoms in the chain were used in this work. The average size of the particles was 10 μm, the pore diameter was 100 Å, and the specific surface was 300 m^2/g. Suspensions with a mass part of the particles of 15 and 30% were prepared in the experiment.

Stable nitroxyl radicals with different structures, charges, and solubility in water (Fig. 1) were used as spin probes. The MK5 radical was synthesized by A.B. Shapiro et al. [18]; 5-DSA and 16-DSA were purchased at Sigma-Aldrich (Germany); positively charged Cat-8, Cat-12, and Cat-16 radicals (counterion Br^-) were kindly provided by Dr. Sci. G.B. Khomutov (Physics Faculty, Moscow State University).

The C-2, C-8, and C-18 hydrophobic microparticles were wetted by ethanol, and then the solution of the spin probe in the borate buffer (pH 8.8) in the case of MK5, 5-DSA, and 16-DSA radicals or the water solution of the probe (for Cat-8, Cat-12, and Cat-16 radicals) was added. The final radical concentration was 2×10^{-4} M. The volumetric parts of the buffer (bidistilled water) and ethanol in a mixture were 58.8 and 41.2%, respectively. After intensive stirring, an aliquote 20 μl was taken from the suspension and put in a capillary for electron paramagnetic resonance (EPR) measurements (the internal diameter of the capillary was 1 mm). Control solutions in a buffer (bidistilled water)/ethanol mixture of the same composition as for the suspensions were prepared for all spin probes.

The samples without the solvent were prepared as follows. The suspension of particles was put on a glass plate, weighed (Scientech, accuracy of 0.1 mg), and left in air at room temperature for 24 h. Weighing and drying in air were repeated until the weight of the plate did not change within the accuracy of the measurements.

A batch of the dried sample (10 mg) was put in a capillary for the EPR measurements (the internal diameter was 1.2 mm) and the initial EPR spectra were recorded. The input of water and ethanol vapors to the dried particles was performed directly in the capillaries for the EPR measurements. To this end, 8 μl of the water–ethanol mixture (58.8% and 41.2% v/v) were added to the upper part of the capillary with the sample so that the distance between the dry sample and the liquid phase was 30 mm; then the capillary was tightly closed with parafilm. Then the capillaries were placed in an exsiccator at a temperature of 35°C for 4 h. The samples were left for an hour at room temperature after being kept in the exsiccator; then the EPR spectra were recorded. The amount of the liquid phase in the capillary decreased by approximately 15% (1.2 μl) up to the moment at which the spectrum was measured.

The amounts of the mixture components in the gas phase can be approximately estimated from the reference data on the partial pressures in the ethanol–water mixture with an ethanol content of 20 mole % (the mixture used in this work contained 17.6 mole % of ethanol) [19]. At 40°C, the partial pressures of the water and ethanol vapors were 0.063 and 0.057 atm, respectively. An estimation of the water and ethanol amount in the gas phase with the use of the Mendeleev–Clapeyron equation shows that their total volume recalculated to the liquid phase does not exceed 0.01 μl; i.e., the reduction of the amount of the liquid phase by 1.2 μl is wholly due to its sample recondensation. It is natural to think that the composition of the condensate on the particles is similar to the composition of the added mixture. Then, on the basis of the volume of the condensate 1.2 μl and the surface area of 3 m^2 for the 10-mg batch of particles, the degree at which the sample surface is filled with water and alcohol is 0.013 and 0.0028 mM/m^2, or 7.8 and 1.7 molecules/nm^2, respectively.

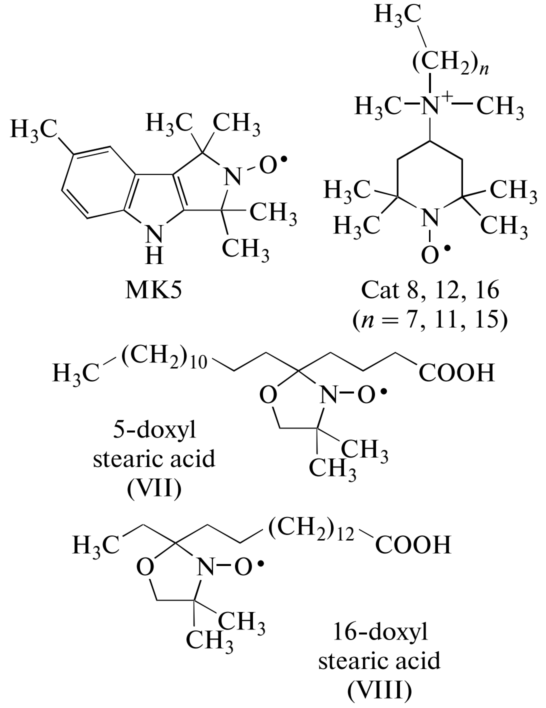

Fig. 1. Chemical structures of the nitroxyl spin probes.

The EPR spectra were recorded on an ER-200D spectrometer (Bruker) using temperature control with an accuracy of ±0.5°C. The EPR spectra linear in the microwave field were recorded at low microwave power ($P = 18$ dB, $H_1 \cong 0.0625$ G) and a low modulation amplitude excluding the spectrum distortion.

For the 5-DSA and 16-DSA spin probes, the EPR spectra were simulated in the model of nonspherical (anisotropic) rotation in the anisotropic medium. In this model, the spin probe is characterized by the coefficients of the rotational diffusion around the symmetry axis ($R_{\parallel}$) of the molecule and the axes perpendicular to it ($R_{\perp}$), the β angle between the z axis of the magnetic tensors (A, g), and the symmetry axis of the diffusion tensor and the order parameter D_{20}:

$$D_{20} = \left\langle \frac{3\cos^2\theta - 1}{2} \right\rangle, \tag{1}$$

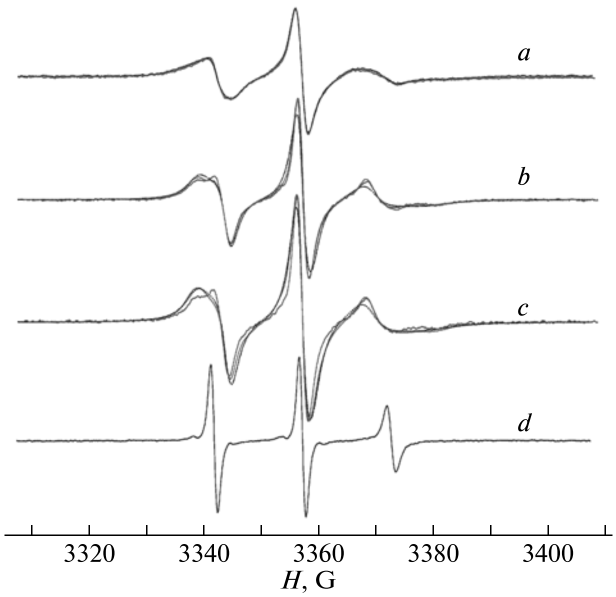

Fig. 2. EPR spectra of the 5-DSA radical in the suspensions of the (*a*) C-2, (*b*) C-8, and (*c*) C-18 particles and in (*d*) the buffer–ethanol mixture. Solid lines are the experimental spectra in 15% (—) and 30% (····) suspensions; the dotted line shows the result of simulation with the use of the program [20] and the nonlinear least-squares method.

where θ is the angle between the symmetry axis of the diffusion tensor and the axis of the local anisotropy of the medium. A program [20] was used for this simulation in which these parameters and the individual line widths were determined by using the nonlinear least-squares method and the Levenberg–Marquardt algorithm. To characterize the rotational dynamics of the spin probes, the correlation times in the model of the isotropic rotation were also determined from the EPR spectra using the relation [21]

$$\tau_{\text{eff}} = 6.65 \times 10^{-10} \Delta H_{+1}((I_{+1}/I_{-1})^{1/2} - 1), \qquad (2)$$

where $I_{\pm 1}$ are the amplitudes of the components of the hyperfine structure (HFS), $m = \pm 1$, and ΔH_{+1} is the width between the extrema of the low-field HFS component.

The polarity of the environment of the spin probes in solution was characterized by the constant of the isotropic HFS on the N^{14} nucleus *s* and the dimensionless parameter *h* [22]

$$h = \frac{a_{\text{W}} - a}{a_{\text{W}} - a_{\text{T}}}, \qquad (3)$$

where a, a_{W}, a_{T} are the a_{iso} values in the suspension of microparticles in water and toluene, respectively. The *h* value is 1 and 0 in the hydrophobic (toluene) and polar (water) environment, respectively.

The spin exchange of nitroxyl probes with paramagnetic Ni^{2+} ions in suspensions of the silica gel microparticles was studied by measuring the additional relaxation broadening of the HFS components of the EPR spectra of probes ($\Delta\Delta H_{pp}$) in the presence of the different concentrations of nickel chloride. The spin exchange rate constants were determined from the slope of the linear dependences of the width of the $m = +1$ component according to the formula [23]

$$k_{\text{ex}} = \frac{\sqrt{3}}{2}\gamma_e \Delta\Delta H_{pp}/c, \qquad (4)$$

where γ_e is the gyromagnetic ratio of the electron and $\Delta\Delta H_{pp}$ is the difference between the line width of the $m = 0$ component in the presence and absence of the paramagnetic ions with the concentration *c*.

RESULTS AND DISCUSSION

The spin probes were chosen according to the following considerations. The MK5 probe (the spin-labeled indole analog) can simulate the behavior of the fluorescent sensor molecule since it contains a fluorescent aromatic indole residue [14]. The 5-DSA and 16-DSA and Cat-8, Cat-12, and Cat-16 spin probes can simulate the behavior of the hydrocarbon chains on the silica gel surface. 5-DSA and 16-DSA are widely used to study the dynamics of lipid membranes, micelles, and emulsions of surface-active compounds [11, 12, 24]. They are sensitive not only to the rotational dynamics and polarities of the environment of the probe, but also to the ordering degree of the hydrocarbon chains. The Cat-8, Cat-12, and Cat-16 probes have linear hydrocarbon chains of different lengths and a positive charge on the nitrogen atom; thus they are sensitive to the electrostatic potential of the surface [25].

5- AND 16-DOXYL STEARATES

EPR spectra of the 5-DSA probe in suspensions of the C-2–C-18 particles (whose weight part of particles are 15 and 30%) and in the buffer solution are given in Fig. 2.

Note first of all that the EPR spectra for 15 and 30% suspensions are close to each other for both probes and all three types of the particles. Taking into account the sharp differences in the form of the spectra of free probes and those coupled with the shell as well, it is possible to conclude that almost all spin probes are built in into the hydrocarbon shells of the microparticles.

Figure 2 shows the best simulation spectra calculated using the program of Budil et al. [20]. Table 1 presents the parameters of the rotational mobility of the simulation spectra. A satisfactory agreement between the experimental and simulation spectra for C-2 particles was achieved only by introducing the partly averaged components of the HFS tensor (*A*) and *g*-tensor (*g*), as opposed to the initial components, which were measured at 77 K. This averaging corresponds to the physical model, where the spin probe has two types of motion: (1) fast libration limited in ampli-

Table 1. Coefficients of the rotational diffusion around the long axis ($\log R_{\parallel}$), short axes ($\log R_{\perp}$), orientation ordering (D_{20}), fitting parameters of the calculated and experimental spectra ($\mathrm{Re}d\chi^2$ and $\mathrm{Re}\sin d$, respectively, see [20]), the angle between the z axes of the magnetic tensors and the tensor of the rotational diffusion (β), and the parameters of the hydrophobicity of the environment (h) of the 5-DSA and 16-DSA spin probes on the C-2, C-8, and C-18 particles

Probe	Particles	$\log R_{\parallel}$	$\log R_{\perp}$	D_{20}	$\mathrm{Re}d\chi^2$	$\mathrm{Re}\sin d$	β, degree	h
5-DSA	C-2	7.98	10.35	0	83.4	0.179	0	0.53
	C-8	8.03	6.73	0.216	212	0.17	0	0.84
	C-18	8.0	6.6	0.223	152	0.12	0	0.80
16-DSA	C-2	8.56	6.14	0.052	134	0.131	90	0.47
	C-8	8.79	5.3	0.057	44	0.124	90	0.56
	C-18	8.74	7.75	0.067	220	0.12	90	0.53

Note: The values of $R_{\parallel}$, $R_{\perp}$, D_{20}, and β were obtained by spectral simulation. The angle β was fixed during simulation. The h values were calculated from the experimental spectra according to formula (3). Toluene was used as a reference hydrophobic solvent. The average errors in the determination of the dynamics parameters were, for $\log R_{\perp}$, $\pm 5 \times 10^{-4}$, $\log R_{\parallel}$ $\pm 4 \times 10^{-2}$; for 5-DSA, $\pm 1 \times 10^{-5}$; and, for 16-DSA, $\pm 1.4 \times 10^{-4}$. The average relative error in the determining parameter h was 6%.

tude leading to the averaged tensors A and g and (2) slower diffusion rotation described by the model [20].

Magnetic tensors averaged over librations are determined from equations [26]

$$\bar{A}_{\parallel} = a_{\mathrm{iso}} + (2/3)\left[A_{zz} - \frac{1}{2}(A_{xx} + A_{yy})\right]S, \qquad (5)$$

$$\bar{A}_{\perp} = a_{\mathrm{iso}} - (1/3)\left[A_{zz} - \frac{1}{2}(A_{xx} + A_{yy})\right]S, \qquad (6)$$

where $S = \left\langle \frac{3\cos^2\theta - 1}{2} \right\rangle$; the angle θ characterizes the angular amplitude of librations averaged over the libration motion.

The $\bar{A}_{\parallel}$, $\bar{A}_{\perp}$ values and analogous quantities for the g tensor were inserted into the program by varying the S value to obtain the best agreement with the experimental spectrum. The optimal S value for the 5-DSA spectrum on the C-2 particles was 0.65, which corresponds to the averaged amplitude $\theta \cong 29°$.

Table 1 also shows that, for C-2 particles, the orientation ordering is absent, but there is a very fast rotation around the long axis of the 5-DSA ($R_{\parallel}$) molecule.

There is significant orientation ordering in the motion of 5-DSA in the shell of the C-8 and C-18 particles, although the order parameter D_{20} is much less than typical values for the one-component lipid membranes and microemulsions (0.4–0.7) [24, 27]. Though the carboxyl group of the 5-DSA probe at pH 8.8 is ionized and localized on the interface with the solvent, the interface itself (in contrast, for instance, to emulsions) is probably not formed due to the absence of the surface-active (polar) groups and fluctuates in the space leading to small D_{20} values.

The experimental and best simulation EPR spectra of the 16-DSA probe on the C-2–C-18 particles are shown in Fig. 3. Table 1 presents the parameters of the rotational dynamics of this probe obtained from the spectral simulations. Similarly to 5-DSA, the form of the spectra in the presence of particles strongly differs from the spectra of these probes in the buffer solution. First, Table 1 shows that the best simulation is obtained at the angle between the symmetry axis of the tensor of the rotational diffusion and the Z axis of 90° (rather than 0°, like for the lipid membranes). This means that the hydrocarbon chain of 16-DSA has a bent conformation. Secondly, there is a slight ordering of the hydrocarbon chains; moreover, the order parameter D_{20} decreases upon the transition from C-18 and C-8 to C-2. The rotational mobility around the short axes ($R_{\perp}$) is almost the same on the C-8 and C-18 particles, and it also decreases on the C-2 particles. These

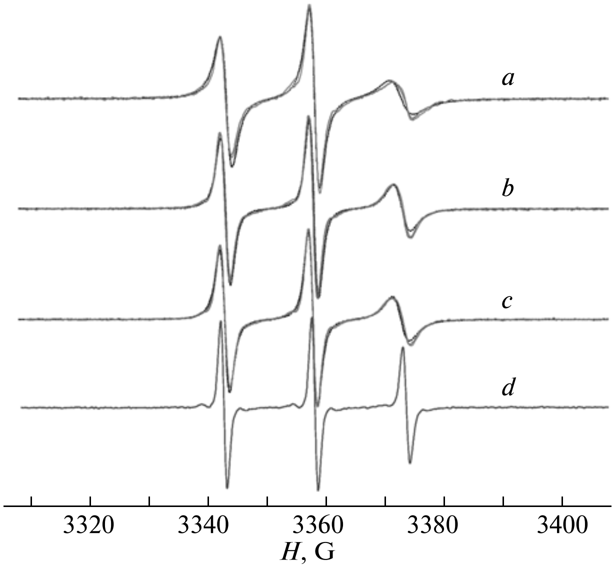

Fig. 3. EPR spectra of the 16-DSA radical in the suspensions of the (*a*) C-2, (*b*) C-8, and (*c*) particles and in (*d*) the buffer–ethanol mixture. Solid lines are experimental spectra in 15% (—) and 30% (····) suspensions; the dotted line shows the result of simulation with the use of the program [20] and nonlinear least-squares method.

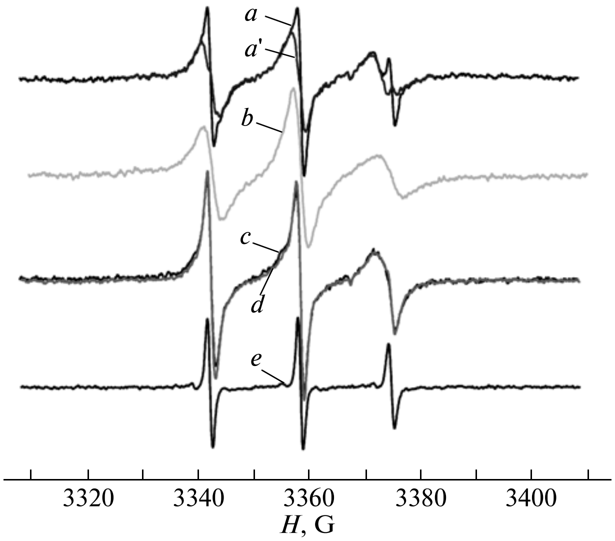

Fig. 4. EPR spectra of the MK5 radical in suspensions of the C-2 particles ((*a*) initial spectrum and (*a*') after the subtraction of the signal of the free probe in the solution), (*b*) C-2 particles in the presence of 60 mM $NiCl_2$, (*c*) C-8 particles, (*d*) C-18 particles, and (*e*) in the buffer–ethanol mixture.

results show that the dynamics of the 16-DSA probe on the C-2 particles depends on the vicinity of the solid surface, which leads not only to the slowing down of its rotation around the short axes ($R_\perp$), but also to the reduction of its orientation ordering. This conclusion correlates well with the above data for the 5-DSA probe.

SPIN-LABELED INDOLE ANALOG

The EPR spectra of the MK5 probe in suspensions of the C-2, C-8, and C-16 particles suspended in the water–alcohol buffer in a concentration of 15 wt % and in the same buffer in the absence of the particles are given in Figs. 4, spectra *a*–*d*. It is seen that spectra *a*–*g* differ strongly from spectrum *d*. In the case of particles with the labeled C-2 phase, two components are seen in the spectrum, one of which corresponds to the free probes in the buffer and the other, a broader component, obviously refers to the probes adsorbed on the particles (Fig. 4, spectrum *a*). Subtracting the signal from the free probes from the total spectrum allows one, in principle, to obtain the spectrum of the adsorbed state. However, the subtraction procedure leads to the appearance of distortions on the $m = -1$ component, as can be seen in Fig. 4, spectrum *a*. We have established that the origin of these distortions is the somewhat larger width of the $m = -1$ component of the unbound probes in the total spectrum when compared with that in the spectrum of these probes in the absence of particles. This additional broadening (δH) is probably due to the chemical exchange between the adsorbed and free state [25]. In frequency units, it corresponds to the exchange velocity $f = 1/\gamma_e \delta H \cong 10^6$ s^{-1}.

The EPR signal of the adsorbed probes is strongly broadened probably due to the heterogeneity of the adsorption locations. In fact, the widths of the $m = \pm 1$ components are 3.3 and 3.7 G, respectively, while the correlation time of the rotation determined according to formula (2) is 0.8 ns. This corresponds to the Lorentz rotational broadening (ΔH_L) being less than 1 G; herewith, the Gauss inhomogeneous broadening (ΔH_G) due to methyl groups does not exceed 1.5 G [12]. Thus, the width of the Gauss–Lorentz convolution $\sqrt{\Delta H_G^2 + 0.25\Delta H_L^2}$ [28] should not exceed ≈1.6 G. It should be noted that, in spite of the relatively high rotational mobility of the probe on the surface, no averaging of this heterogeneity for the characteristic time ~10^{-7} s occurs.

The a_{iso} value characterizing the hydrophobicity of the environment of the MK5 probe is 15.65 G, while it is 16.2 G in the buffer in the absence of the particles; i.e., the environment of the MK5 probe in the labeled C-2 phase, which is two C–C bonds thick, is much more hydrophobic than that in the surrounding solution. It is possible to suppose that the MK5 probe is either oriented by the NO group to the particle surface or rests upon this surface so that the NO group is immersed in the hydrocarbon phase.

To specify the degree of availability of the contents of the hydrocarbon shell for the water-soluble compounds, the action of the paramagnetic relaxant nickel chloride on the spin probes was studied. The EPR signal from the free probes in the disperse medium of the suspension broadened to its complete disappearance in the presence of 60 mM $NiCl_2$ (the same as in the control experiments in the absence of particles). However, the exchange broadening of the HFS component of the EPR signal of the adsorbed radicals at 60 mM, and even at 100 mM $NiCl_2$, was almost absent. This result shows that the reporter group of the MK5 radical is inaccessible for the water-soluble agents, even in the case of a thin hydrocarbon shell of the C-2 particles. The correlation time of the rotation of the MK5 probe calculated from the spectrum measured in the presence of 60 mM $NiCl_2$ is 1.1 ns.

The MK5 spectra in the presence of the C-8 and C-18 particles nearly coincide (Fig. 4, spectra *c*, *d*): in the case of C-8, the signal of the adsorbed radical is more broadened and the contribution of the adsorbed radical is larger than that for the C-18 particles, as is shown by the spectral subtraction. The a_{iso} values for the C-8 and C-18 particles are 15.9 and 15.7 G, respectively; i.e., taking into account the errors contributed at the spectral subtraction, the hydrophobicity of the MK5 environment on these particles is the same as that on C-2.

POSITIVELY CHARGED Cat-8, Cat-12, AND Cat-16 RADICALS

The EPR spectra of all Cat radicals in the presence of the C-2, C-8, and C-18 particles correspond to the region of fast rotations. Table 2 presents the correlation times of the rotation and the hydrophobicity parameters of the environment for these probes on all particles and in the buffer solution–ethanol mixture. It is possible to notice the following regularities in the dynamics and polarity of the environment of these probes: (1) the rotational times in the buffer have almost no dependence on the length of the radical hydrocarbon chains and are 0.09–0.1 ns. In the presence of particles, the correlation times increase 6–14 times and depend on the length of the hydrocarbon chain of both the spin probe and alkyl groups covalently bound to the silica gel surface. The τ_{eff} values increase from 0.5–0.6 ns for Cat-8 to 1.3 ns for Cat-16 with an increase in the length of the hydrocarbon tail of the probe.

The change in the τ_{eff} value with the thickness of the hydrocarbon shell on the surface of the particles probably depends on the length of the tail of the spin probe itself: for Cat-8, the τ_{eff} value remains almost unchanged; for Cat-12, it slightly increases; and for Cat-16, it decreases upon a transition from C-2 to C-8 and C-18 particles. The hydrophobicity of the environment of all three spin probes increases in the series C-2 < C-8 < Cat-18.

The character of all these changes can be qualitatively explained as follows. The increase in the rotational correlation time of the Cat spin probes in the presence of particles (on average by an order of magnitude) shows that all spin probes are included in hydrocarbon shells of the C-2, C-8, and C-18 particles. If, in the buffer, the high rotational mobility of the reporter group was determined by its rotation around the several nearest single bonds and did not depend on the length of the hydrocarbon tail of the probe, then the reporter probe groups on the particles are immersed into the lipid shell with a very high viscosity and both the reorientation of the hydrocarbon tails and the dynamics of the matrix contribute to the reorientation speed of the reporter group. It should be noted, however that the rotational mobility of all Cat radicals remains quite high and, even for the C-2 particles, does not slow down near the surface, as is observed for the same probes upon an interaction with the levasil nanoparticles [25]. Therefore, it is possible to conclude that the surface of such particles does not contain negative charges or these charges are inaccessible for the positively charged polar head of the Cat probe.

Table 2. Hydrophobicity parameters of the environment (h) and the correlation times of the rotation (τ_{eff}) for the Cat-8, Cat-12, and Cat-16 spin probes on the C-2, C-8, and C-18 particles

Probe	Particles	h	τ_{eff}, ns
Cat8	C-2	0.46	0.61
	C-8	0.55	0.51
	C-18	0.65	0.6
Cat12	C-2	0.61	0.76
	C-8	0.66	0.8
	C-18	0.735	0.85
Cat16	C-2	0.61	1.3
	C-8	0.71	0.9
	C-18	0.735	0.9

Note: The τ_{eff} and h values were calculated from the experimental spectra according to the formulas (2) and (3), respectively. Octanol was used as a reference hydrophobic solvent. The average relative errors in the determination of the τ_{eff} and h parameters were 6% and 5%, respectively.

THE EFFECT OF REMOVING THE SOLVENT ON MOLECULAR DYNAMICS IN THE HYDROCARBON SHELL

Thus, these data show that the spin probes, which can simulate different types of analytes or sensors, have high rotational and conformation mobility in the hydrocarbon shell of the Silasorb microparticles which are in equilibrium with the solution.

Due to the possible usage of these particles as matrices for detecting gaseous molecules, it is of high interest to study the molecular mobility in the shell of microparticles in the absence of the solvent. For this purpose, the solvent was removed from the suspension as described in Materials and Methods. The examples of the EPR spectra of the lipid 5-DSA and 16-DSA spin probes on the dry particles are given in Fig. 5. Figure 5 shows that these spectra differ drastically from the spectra of suspensions: they correspond to the region of slow rotations, as opposed to the region of fast rotations for the particles, which are in equilibrium with the solution. The values of the $2A'_{zz}$ parameter characterizing the frequency (or the angular amplitude) of rotations are given in Table 3. First, Table 3 shows that in both probes the $2A'_{zz}$ values increase with an increase in shell thickness. Second, the $2A'_{zz}$ values for 16-DSA are noticeably less than those for 5-DSA. The comparison with the limiting values of these parameters for both probes from literature [11, 24, 27] shows that the correlation times of the rotation of the spin probes are $\geq 10^{-7}$ s; i.e., they increase by at least two orders of magnitude when the solvent is removed. The differences in the mobility of the 5-DSA and 16-DSA probes in the dried samples correlate with the differences on the particles in the presence of the solvent, as well as with the differences

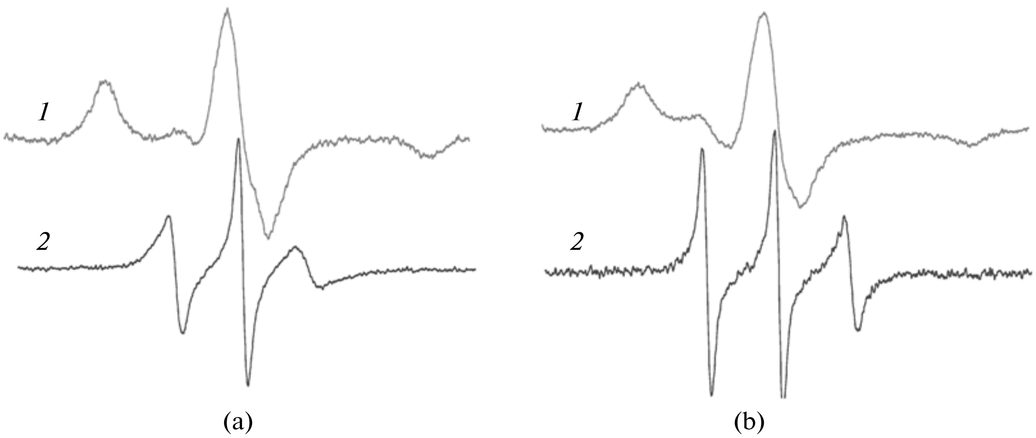

Fig. 5. EPR spectra of (a) 5-DSA and (b) 16-DSA (*1*) after drying the suspensions of the C-8 particles in air under room temperature and (*2*) after incubation of the dry sample with the C-8 particles in the buffer–ethanol vapors. Concentration of the spin probe, 1.2×10^{-4} M. The buffer : ethanol ratio is 58.8% : 41.2% v/v.

in the lipid membranes. Therefore, they are probably due to the different localizations of the reporter NO group of these probes: in the case of 16-DSA, it is probably located closer to surface and further from the polar head of the probe.

THE EFFECT OF THE SOLVENT VAPORS ON THE MOLECULAR DYNAMICS IN THE HYDROCARBON SHELL

Upon admitting the solvent vapors to the dried C-8 particles and keeping them for 4 h in the atmosphere of these vapors, the 5-DSA and 16-DSA spectra take the form shown in Fig. 5. It is seen that the mobility of both probes sharply increases and corresponds to the nanosecond range of the correlation times (1.4 and 0.79 ns, respectively), the same as for suspensions in the ethanol–water mixture. However, the form of the spectra is not recovered completely, as can be seen from comparing Fig. 5 with Figs. 2 and 3. For the 5-DSA radical, the anisotropy of the spectrum disappears after drying and the subsequent input of vapors, indicating the orientation ordering, and a certain heterogeneity appears (see the overlapping of signals in the $m = +1$ component). For 16-DSA, the rotational correlation times in the initial suspension and after the input of vapors almost coincide: 0.75 and 0.79 ns, respectively. However, the line widths in the second case are higher, which also indicates a certain heterogeneity of the probe mobility. The differences in the spectral parameter before and after drying and the subsequent input of vapors is obviously due to the difference in the amount of solvent, which is enough in the first case and not enough in the second case for the complete and homogeneous solvation of the hydrocarbon chains. However, it is important to note the appearance of a high rotational mobility of the probes (and, obviously, hydrocarbon chains themselves) in the presence of the solvent vapors, which should considerably affect the functioning of sensors on the basis of these matrices.

Table 3. Mobility parameters $2A'_{zz}$ of the 5-DSA and 16-DSA spin probes on the C-2, C-8, and C-18 particles in the absence of solvent

Probe	Particles	$2A'_{zz}$, G
5-DSA	C-2	67.85 ± 0.05
	C-8	69.45 ± 0.15
	C-18	69.8 ± 0.1
16-DSA	C-2	65.6 ± 0.1
	C-8	68.4 ± 0.1
	C-18	68.5 ± 0.2

CONCLUSIONS

Thus, it was shown in this work that the hydrocarbon shell of the Silasorb silica gel microparticles in the presence of the solvent provides both high rotational and conformational mobility and a very high environmental hydrophobicity for the molecules introduced in it. The regularities were established in the change of the rotational mobility, orientation ordering, and hydrophobicity of the environment, depending on the thickness of the hydrocarbon shell, for the probes of different structures: the radical containing an aromatic fragment simulating fluorophores; lipid spin probe sensitive to the microviscosity of the lipid environment, and charged probes sensitive to electrostatic interactions. It was shown that the rotational mobility of the lipid spin probes in the hydrocarbon shells sharply decreases after the removal of the solvent and is restored in the presence of water and ethanol vapors. The high rotational mobility of the spin probes and the very high hydrophobicity of their environment in the shell of the microparticles in the liquid phase and the solvent vapors allow one to conclude that the Silasorb microparticles are a perspective matrix for producing molecular chemosensors on analytes in solutions and the gas phase.

ACKNOWLEDGMENTS

This work was supported by State Contract no. 02.740.11.0113.

REFERENCES

1. W. Jin and J. D. Brennan, "Properties and Applications of Proteins Encapsulated within Sol–Gel Derived Materials," Anal. Chim. Acta 461, 1–36 (2002).
2. A. C. Pierre, "The Sol–Gel Encapsulation of Enzymes," Biocatal. Biotransform. 22, 145–170 (2004).
3. G. Hungerford, A. Rei, M. I. C. Ferreira, K. Suhling, and C. Tregidgo, "Diffusion in a Sol–Gel-Derived Medium with a View toward Biosensor Applications," J. Phys. Chem. 111, 3558–3562 (2007).
4. A. Burns, P. Sengupta, T. Zedayko, B. Baird, and U. Wiesner, "Core/Shell Fluorescent Silica Nanoparticles for Chemical Sensing: Towards Single-Particle Laboratories," Small 2, 723–726 (2006).
5. A. van Blaaderen and A. Vrij, "Synthesis and Characterization of Monodisperse Colloidal Organo-Silica Spheres," J. Colloid Interface Sci. 156, 1–18 (1993).
6. W. Stoeber, A. Fink, and E. Bohn, "Controlled Growth of Monodisperse Silica Spheres in the Micron-Size Range," J. Colloid Interface Sci. 26, 62–69 (1968).
7. A. Burns, H. Ow, and U. Wiesner, "Fluorescent Core–Shell Silica Nanoparticles: Towards "Lab on a Particle" Architectures for Nanobiotechnology," Chem. Soc. Rev. 35, 1028–1042 (2006).
8. T. Akiyama, T. Hishiya, H. Asanuma, and M. Komiyama, "Molecular Imprinting of Cyclodextrin on Silica–Gel Support for the Stationary Phase of High-Performance-Liquid-Chromatography," J. Inclusion Phenom. Macrocyclic Chem. 41, 149–153 (2001).
9. D. V. Shamshurin, E. N. Shapovalova, and O. A. Shpigun, "Chromatographic Characteristics of the Silica Gels Modified with Chitosan and Its Derivatives," Vestn. Mosk. Univ., Ser. 2: Khim. 45, 180–185 (2004).
10. N. A. El'tekova and Yu. A. El'tekov, "Adsorption of Aromatic Compounds from Solutions in n[italic]-Heptane by Modified Nanoporous Silica," Zh. Fiz. Khim. 81 (1), 83–87 (2007) [Russ. J. Phys. Chem. A 81 (1), 78–82 (2007)].
11. L. Berliner, in Spin Labeling: Theory and Applications, Ed. by L. Berliner (Academic, New York, United States, 1976; Mir, Moscow, 1979).
12. Biological Magnetic Resonance, Ed. by L. Berliner and J. Reuben, Vol. 8: L. Berliner, in Spin Labeling: Theory and Applications, Ed. by L. Berliner (Plenum, London, 1989), Part 1.
13. Biological Magnetic Resonance, Vol. 22: O. Grinberg, in Very High-Frequency ESR/EPR, Ed. by O. Grinberg and L. Berliner (Kluwer, New York, United States, 2004).
14. V. A. Livshits, B. G. Dzikovskii, V. G. Avakyan, E. A. Samardak, E. Yu. Polyakova, V. Yu. Rudyak, and M. V. Alfimov, "Inclusion Complexes of Spin-Labeled Indoles with Cyclodextrins in Aqueous Solutions," Izv. Akad. Nauk, Ser. Khim., No. 5, 1139–1147 (2006) [Russ. Chem. Bull. 54 (5), 1169–1177 (2006)].
15. V. A. Livshits, B. G. Dzikovskii, E. A. Samardak, and M. V. Alfimov, "Guest–Host Complexes of Spin-Labeled Indoles with Cyclodextrins in the Solid Phase: An ESR Study," Izv. Akad. Nauk, Ser. Khim., No. 2, 233–241 (2006) [Russ. Chem. Bull. 55 (2), 238–246 (2006)].
16. V. A. Livshits, I. V. Demisheva, B. G. Dzikovskii, V. G. Avakyan, and M. V. Alfimov, "Structure and Molecular Dynamics of the Ternary Complexes of Cyclodextrins with Spin-Labeled Indoles and Hydrocarbons in the Solid Phase: ESR Spectroscopy and Quantum-Chemical Calculations," Izv. Akad. Nauk, Ser. Khim., No. 12, 2081–2093 (2006) [Russ. Chem. Bull. 55 (12), 2161–2173 (2006)].
17. B. Dzikovski, D. Tipikin, V. Livshits, K. Earle, and J. Freed, "Multifrequency ESR Study of Spin-Labeled Molecules in Inclusion Compounds with Cyclodextrins," Phys. Chem. Chem. Phys. 11, 6676–6688 (2009).
18. A. B. Shapiro, B. V. Rozanov, E. G. Rozantsev, N. F. Kucherova, L. A. Aksanova, and N. N. Novikova, "Mass-Spectrometric Study of New Stable Iminoxyls of the Indole Class," Izv. Akad. Nauk SSSR, Ser. Khim., No. 4, 867–870 (1974) [Bull. Acad. Sci. USSR, Div. Chem. 20 (4), 784–786 (1974)].
19. Chemist's Handbook, Ed. by B. P. Nikol'skii (Khimiya, Moscow, 1964), Vol. 3 [in Russian].
20. D. E. Budil, S. Lee, S. Saxena, and J. H. Freed, "Non-Linear Least-Squares Analysis of Slow-Motion EPR Spectra in One and Two Dimensions Using a Modified Levenberg–Marquardt Algorithm," J. Magn. Reson., Ser. A 120, 155–189 (1996).
21. A. M. Vasserman and A. L. Kovarskii, Spin Labels and Probes in the Physical Chemistry of Polymers (Nauka, Moscow, 1986) [in Russian].
22. A. N. Kuznetsov, Spin Probe Method (Nauka, Moscow, 1976) [in Russian].
23. K. I. Zamaraev, Yu. N. Molin, and K. M. Salikhov, Spin Exchange (Nauka, Novosibirsk, 1977; Springer, Berlin, 1980).
24. B. G. Dzikovski and V. A. Livshits, "EPR Spin Probe Study of Molecular Ordering and Dynamics in Monolayers at Oil/Water Interfaces," Phys. Chem. Chem. Phys. 5, 5271–5278 (2003).
25. V. A. Livshits, I. V. Demisheva, B. B. Meshkov, V. P. Tsybyshev, and M. V. Alfimov, "A Study of Adsorption and Molecular Dynamics of Spin-Labeled Molecules on the Surface of Silica Nanoparticles," Ross. Nanotekhnol. 4 (1–2), 51–61 (2009) [Nanotechnol. Russ. 4 (1–2), 45–54 (2009)].
26. L. Berliner, in Spin Labeling: Theory and Applications, Ed. by L. Berliner (Academic, New York, United States, 1976; Mir, Moscow, 1979), Vol. 1, Chap. 12.
27. M. D. Reboiras and D. Marsh, "EPR Studies on the Influence of Chainlength on the Segmental Motion of Spin-Labelled Fatty Acids in Dimyristoylphosphatidylcholine Bilayers," Biochim. Biophys. Acta 1063 (2), 259–264 (1991).
28. Ya. S. Lebedev and V. I. Muromtsev, EPR and Relaxation of Stabilized Radicals (Khimiya, Moscow, 1972) [in Russian].